

Techno-Economic Optimization of Cellulose Corrugated Pads for Evaporative Cooling Systems Using the Net Saving Method

www.rericjournal.ait.ac.th

Nitipong Soponpongpipat*, 1, Supanut Taengcharoensuk*, Pongsiri Jaruyanon*

Abstract – This study develops a mathematical model to determine the optimum thickness of cellulose corrugated wetted pads in direct evaporative cooling systems by integrating heat transfer, airflow pressure drop, and total system cost. The model was validated against experimental data, achieving a minimum RMSE of 1.22 °C and a MAPE of 4.01%, confirming high predictive accuracy. Results show a U-shaped relationship between pad thickness and total cost, with an optimum point minimizing the combined expenses of pad material, fan, and pump energy. Sensitivity analysis identified inlet and outlet air temperatures as the most influential factors on optimum thickness. To avoid computationally intensive brute-force optimization, a third-degree polynomial correlation was formulated using saturation effectiveness as the input. The correlation predicted optimum thickness with MAPE below 4% and RMSE below 0.005 m for effectiveness values between 0.45–0.90. However, errors increased significantly beyond 0.90, with MAPE reaching 19.44%. Applicability analysis confirmed the correlation's reliability across conditioned volumes of 15–1,500 m³, air change rates of 10–40 h⁻¹, and cost factors of 0.0090–0.0224, with errors under 12%. While the correlation provides a practical tool for preliminary design, comprehensive cost evaluation remains essential for final optimization.

Keywords – evaporative cooling pad, optimum pad thickness, polynomial regression, saturation effectiveness, techno-economic analysis.

1. INTRODUCTION

The growing emphasis on smart agriculture has highlighted the importance of maintaining optimal environmental conditions for the growth of plants and livestock to enhance productivity. Among various climate control solutions, evaporative cooling systems have gained popularity due to their low energy consumption, simplicity, and affordability [1]-[7]. These systems work by lowering air temperature while simultaneously increasing humidity—features that are particularly beneficial for agricultural applications. The relatively low initial and operating costs make evaporative cooling a viable and energy-efficient option in this context. While evaporative cooling performs best in arid environments, its effectiveness diminishes in humid tropical climates due to the smaller wet-bulb depression (i.e., the difference between dry-bulb and wet-bulb temperatures). Nevertheless, even under hot and humid conditions, well-designed evaporative cooling systems can still reduce air temperatures by several degrees, making them a practical solution when optimized for local conditions [8]-[9]. The key lies in enhancing the performance of the wetted media while minimizing associated energy and material costs.

DOI: https://doi.org/10.64289/iej.25.03A11.1208787

Corresponding author;

Tel +66 34 259025 Fax: +66 34 259025 E-mail: <u>Nitipongsopon@gmail.com</u>

pad, commonly constructed from corrugated sheets bonded with resin to form rigid media with defined flute angles. Pad thicknesses typically range from 5 to 30 cm, include cellulose. materials used polyethylene, fiberglass, carbon fiber, and metal. Rigid media pads offer several advantages over fibrous types, including greater surface area for air-water contact, better structural integrity, and longer service life [10-11]. Pad thickness plays a pivotal role in system performance. It directly influences the appropriate air velocity through the pad, with higher velocities typically leading to reduced saturation effectiveness [9], [12]-[15] and a narrower temperature drop across the pad [16]. Increased airspeed also results in higher pressure drop [17-19], increased water consumption, and higher heat and mass transfer coefficients. While thicker pads generally improve saturation effectiveness [20], they also increase airflow resistance and pressure drop [21]. Beyond a certain point, however, the marginal gains in cooling diminish while material and operating costs continue to rise. This trade-off underscores the need to determine an economically optimal pad thickness rather than simply maximizing technical performance. These findings suggest the existence of an optimum thickness that maximizes cooling efficiency without incurring unnecessary energy or financial penalties.

A critical component in such systems is the wetted

A rational approach to selecting pad thickness must therefore balance performance with cost. Thicker pads increase both capital and operating expenditures-due to higher material, fan, and pump energy requirements—while thinner pads, although cheaper, may compromise cooling performance and increase downstream energy demands. The net saving method

©2025. Published by RERIC in International Energy Journal (IEJ), selection and/or peer-reviewed under the responsibility of the Organizers of the "17th International Conference on Science, Technology and Innovation for Sustainable Well-Being (STISWB 2025)" and the Guest Editor: Prof. Pradit Terdtoon of Chiang Mai University, Chiang Mai, Thailand.

^{*}Department of Mechanical Engineering, Faculty of Engineering and Industrial Technology, Silpakorn University, Nakhon Pathom, 73000, Thailand

offers a systematic framework to evaluate this trade-off [22]. It defines net savings as the difference between the monetary value of performance benefits (e.g., energy savings or enhanced productivity) and the associated costs. The thickness that yields the maximum net savings is identified as the optimal value [23]. This approach has been successfully applied in analogous fields such as optimal insulation thickness in buildings.

This study employs a techno-economic assessment using the Net Saving method to determine the optimum cost-effective thickness of cellulose corrugated evaporative cooling pads under representative tropical climatic conditions. Instead of relying on a specific experimental dataset, the analysis utilizes performance correlations from the literature along with practical economic assumptions. By integrating technical metrics (e.g., cooling effectiveness, airflow, energy use) with economic considerations (pad and energy costs), the framework enables design optimization in humid climates where performance margins are narrow. Additionally, a predictive correlation for optimum pad thickness is proposed to facilitate initial design estimates and reduce reliance on brute-force optimization.

2. MATERIALS AND METHOD

2.1 Mathematical Model

The mathematical model proposed in this work has two major parts: (1) an air heat transfer and pressure drop model for flow through wet pad in an evaporative cooling system, and (2) a cost estimation model. A comprehensive explanation of the formulation for both components is given in the sections that follow.

2.1.1 Heat Transfer and Pressure Drop Model

The first step in the modelling framework involves computing the air mass flow rate through the wetted pad, which is derived from the specified air change rate (ACH) and the volume of the conditioned space, as shown in Equation (1) [24].

$$\dot{m}_{air} = \frac{\rho_{air} * V_{room} * ACH}{3600}$$
 (1)

The inlet air conditions are used to estimate the wet-bulb temperature using the empirical correlation proposed by Stull [25], as given in Equation (2).

$$\begin{split} T_{WB} = & T_i tan^{-1} \left(0.151977 (RH\% + 8.313659)^{1/2} \right) \\ + & tan^{-1} (T_i + RH\%) - tan^{-1} (RH\% - 1.676331) \\ + & 0.00391838* (RH\%)^{3/2} * tan^{-1} (0.023101RH\%) \\ - & 4.686035 \end{split} \tag{2}$$

Once T_{WB} is determined, the saturation effectiveness of the wetted pad can be computed using Equation (3).

$$\varepsilon = \frac{T_{i} - T_{e}}{T_{i} - T_{WB}} \tag{3}$$

Geometric parameters related to the wetted pad include the total heat transfer area, specific surface area, pad volume, cross-sectional area, and characteristic length. These are defined in Equations (4) - (6).

$$A_{w} = A_{s} V_{pad}$$
 (4)

$$V_{pad} = LA_{pad}$$
 (5)

$$L_{e} = \frac{V_{pad}}{A_{w}} \tag{6}$$

The velocity of the air through wetted pad is calculated under the condition that all of the air mass flow rate from Equation (1) flows through the pad without leakage. The velocity is therefore calculated from Equation (7).

$$v = \frac{\dot{m}_{air}}{\rho_{air} A_{pad}} \tag{7}$$

The convective heat transfer coefficient is approximated from empirical correlations in the literature [5], [26] while utilizing Equation (10) for computation of Reynolds number.

$$Nu = \frac{h_e L_e}{k_{air}} = 0.10 \left(\frac{L_e}{L}\right)^{0.12} Re^{0.8} Pr^{1/3}$$
 (8)

$$Nu = 0.172 \left(\frac{L_e}{L}\right)^{0.32} Re^{0.85} Pr^{1/3}$$
 (9)

$$Re = \frac{\rho_{air} vL_e}{\mu_{air}}$$
 (10)

The saturation effectiveness, heat transfer coefficient, and air mass flow rate relationship is determined in accordance with the heat transfer across the wetted surface, as given in Equation (11) [26], [24].

$$A_{w} = \frac{-\dot{m}_{air}c_{p,air}\ln(1-\epsilon)}{h_{c}}$$
 (11)

The pressure drop across the wetted pad is calculated using the correlation developed by He *et al.* [27], as presented in Equation (12) and (13).

$$\Delta P_{\text{drop}} = 0.768 \left(\frac{l_{\text{e}}}{l}\right)^{-0.469} \left(1 + Q_{\text{w}}^{1.139}\right) v^2$$
 (12)

$$Q_{w} = q_{w} A_{pad}$$
 (13)

The central aim of this research is to identify the optimal pad thickness that provides the required saturation effectiveness and, in turn, delivers the desired outlet air temperature. To achieve this, a computational framework is established, as depicted in Figure 1. The model incorporates several input parameters, namely the conditioned space volume, inlet air relative humidity, inlet and outlet dry-bulb temperatures, pad thickness, and specific surface area. Based on these inputs, the air

mass flow rate, wet-bulb temperature, and saturation effectiveness are determined. Within this framework, the total heat transfer area is initially treated as an unknown parameter and is arbitrarily assigned a starting value. This assumed value governs the geometrical dimensions of the wetted pad (Equations 4-6) and subsequently affects the Reynolds number and the convective heat transfer coefficient (Equations 7–10). Once all intermediate quantities are evaluated, the total heat transfer area is recalculated. If the recalculated value differs from the assumed one, the process is iteratively repeated, adopting the updated heat transfer area as the new input. The iteration proceeds until the relative error falls below 0.2%. Ultimately, the pressure drop is evaluated from the air velocity predicted by the model using Equations (12) and (13).

2.1.2 Cost Estimation Model

It is well established that the total cost of a direct evaporative cooling system comprises material costs, equipment costs, operating energy consumption costs, and maintenance expenses. Developing a comprehensive cost model that incorporates all these elements is essential for accurate evaluation. However, when the optimum pad thickness that minimizes the total cost is unknown, it becomes necessary to evaluate the total cost across a range of candidate thickness values and select the one that yields the minimum cost. This brute-force approach can be computationally intensive, particularly when the total cost function is complex. To reduce the computational burden during the preliminary design stage, this study proposes a simplified cost model focused on components directly associated with the wetted pad, including the cost of the pad material and the electricity consumption of the fan and water pump. The total cost function associated with the wetted pad is expressed in Equation (14).

$$Cos t_{total} = Cos t_{pad} + Cos t_{E,fan} + Cos t_{E,pump}$$
 (14)

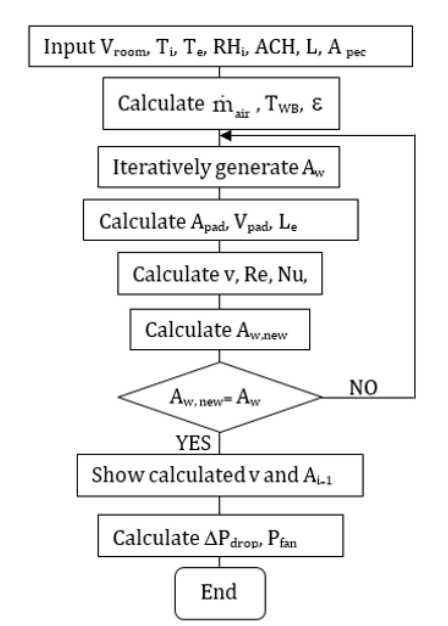


Fig. 1. Calculation flow chart of the first component.

Based on a market survey of cellulose corrugated pads, the material cost was found to vary linearly with the volume of the pad, with a slope coefficient denoted as k_{pad} , as illustrated in Figure 2. Accordingly, the cost of the pad material is modeled by Equation (15).

$$Cos t_{pad} = k_{pad} V_{pad}$$
 (15)

The electricity cost for fan and pump operation is modeled as a linear function of the energy consumed, represented by Equations (16) and (17), respectively.

$$Cos t_{E fan} = k_E E_{fan}$$
 (16)

$$Cos t_{E,pump} = k_E E_{pump}$$
 (17)

The electrical energy demand of the fan and pump is evaluated based on the required fluid power and the corresponding equipment efficiencies, as expressed in Equations (18) and (19).

$$E_{fan} = \frac{vA_{pad}\Delta P_{drop}h}{1000*\eta_{fan}}$$
 (18)

$$E_{pump} = \frac{Q_{w} \Delta P_{drop,w} h}{1000 * 3600 * \eta_{pump}}$$
 (19)

Since k_{pad} and k_E are treated as constants, the ratio between these coefficients over a given period is also constant, and this relationship can be expressed as shown in the equation below.

$$\alpha = \frac{k_E}{k_{pad}} \tag{20}$$

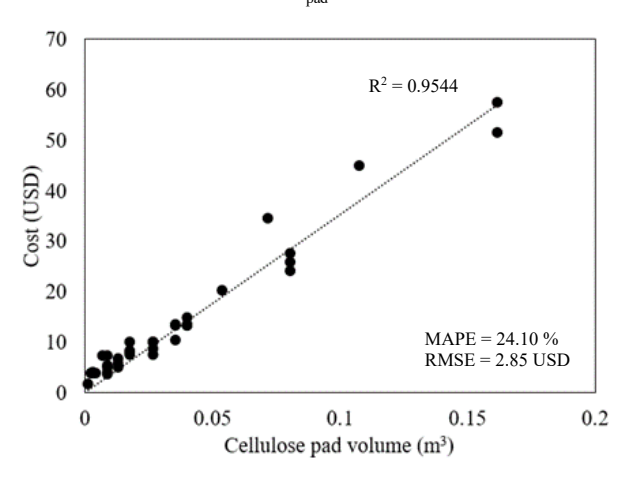


Fig. 2. Cost of cellulose corrugate pad.

By combining Equations (14) - (20), the total cost function can be reformulated.

$$Cos t_{total} = k_{pad} \left(V_{pad} + \alpha E_{fan} + \alpha E_{pump} \right)$$
 (21)

According to the net saving principle, the economically optimal point is defined as the condition at which the difference between the monetary savings and the total cost is maximized. In the present analysis, however, the savings component is not explicitly included; therefore, the optimum point is determined

solely based on the total cost function. The optimum pad thickness, denoted as L_{op} , is obtained by minimizing the total cost function. Since the pad volume (V_{pad}), fan energy consumption (E_{fan}), and pump energy consumption (E_{pump}) are all dependent on the pad thickness, the total cost becomes a function of this variable.

$$\frac{\partial \operatorname{Cost}_{\text{total}}}{\partial L} = \frac{\partial k_{\text{pad}} \left(V_{\text{pad}} + \alpha E_{\text{fan}} + \alpha E_{\text{pump}} \right)}{\partial L} = 0 \quad (22)$$

Therefore, the condition for determining the optimum pad thickness corresponds to the minimization of the total cost function, as expressed in the subsequent equations.

$$V_{pad}\left(L_{op}\right) + \alpha E_{fan}\left(L_{op}\right) + \alpha E_{pump}\left(L_{op}\right) = 0 \tag{23}$$

The use of parentheses in Equation (23) explicitly denotes that V_{pad} , E_{fan} , and E_{pump} are implicit functions of the optimum pad thickness. Consequently, the

optimum pad thickness (Lop) must be determined through a numerical approach.

2.2 Simulation Parameters

To determine the optimal pad thickness that minimizes the overall cost, this study specifies a set of fixed input parameters for numerical analysis. The values employed in the simulation are presented in Table 1, with references provided for parameters adopted from prior research. Since the investigation centers on evaporative cooling systems operating under hot and humid climatic conditions, the inlet air temperature and relative humidity are assigned within representative ranges of 29-33°C and 58-78%, respectively. Furthermore, to examine the influence of critical variables on the optimal pad thickness—namely room volume, air change rate (ACH), pad specific surface area (As), wetbulb depression, and cost factor (α)—these parameters are systematically varied across practical ranges recommended in the literature.

Table 1. Summary of simulation input parameters.

Parameter	Value/Range	Reference
Inlet air temperature	29–33 °C	N/A
Relative humidity	58-78%	N/A
Pad thickness	0.02 - 1.00 m	N/A
Specific surface area	370*, 400*, 420 m ² m ⁻³	*[28]
Conditioned space volume	15–15,000 m ³	N/A
ACH	10–60 h ⁻¹	10–30 h ⁻¹ recommended [29]
Wet-bulb depression	3-6 °C	N/A
Cost factor (α)	0.0090 -0.0449	N/A
Material cost coefficient (kpad)	352.08 USD-m ⁻³	Figure 2
Efficiency (fan and pump)	0.7 (fan), 0.8 (pump)	[30]–[32]
Specific water consumption	$0.28 \text{ m}^3\text{h}^{-1}\cdot\text{m}^2$	[33]
Pad service life	4.5 years	N/A
System operating hours	16 h-day ⁻¹	N/A

2.3 Experimental Validation

The heat transfer model for airflow through the wetted pad was validated using experimental data obtained from a 2.63 m wind tunnel, as shown in Figure 3. A cellulose corrugated pad with a volume of 1.08×10^{-2} m³ and a specific surface area of 400 m² m⁻³ was mounted in the test section. The water flow rate across the pad was adjusted to four levels: 0.3, 0.4, 0.5, and 0.6 kg s⁻¹. The inlet air dry-bulb temperature varied between 30 °C and 33.5 °C, with relative humidity ranging from 59% to 68% RH. Five inlet air velocities were examined: 0.25, 0.657, 0.973, 1.482, and 2.0 m s⁻¹. To maintain steady-state operation, the return water temperature in the reservoir was monitored, and steady-state was assumed once this temperature stabilized. Data acquisition commenced after one hour of steady-state operation. Each test condition was repeated five times, and the results were statistically evaluated at a 95% confidence level. The

outlet temperatures obtained from the experiments were evaluated against the corresponding predictions of the proposed heat transfer model.



Fig. 3. The wind tunnel used in the experiment.

3. RESULTS AND DISCUSSION

3.1 Validation of the Heat Transfer Model

this simulation study, empirical correlations recommended in previous research [5], [16] were adopted, and the predicted results were compared with experimental data under identical conditions. The outlet dry-bulb air temperature predicted using correlation (8) yielded a root mean square error (RMSE) of 1.34 °C and a mean absolute percentage error (MAPE) of 4.50%, as illustrated in Figure 4. The data distribution indicates a slight underprediction compared to the experimental measurements. When correlation (9) was applied, the prediction improved slightly, with an RMSE of 1.22 °C and a MAPE of 4.01%, as shown in Figure 5. A similar underprediction trend was observed. This consistent underestimation may be attributed to the measurement uncertainty associated with the temperature sensors. The experiment employed type-K thermocouples and a digital display unit, both having a measurement uncertainty of ±1 °C, which is comparable to the RMSE values observed in both cases. These findings confirm that both correlations provide valid approaches for modeling the heat transfer process. However, since correlation (9) provides slightly better accuracy, it is adopted for all subsequent simulations in this study.

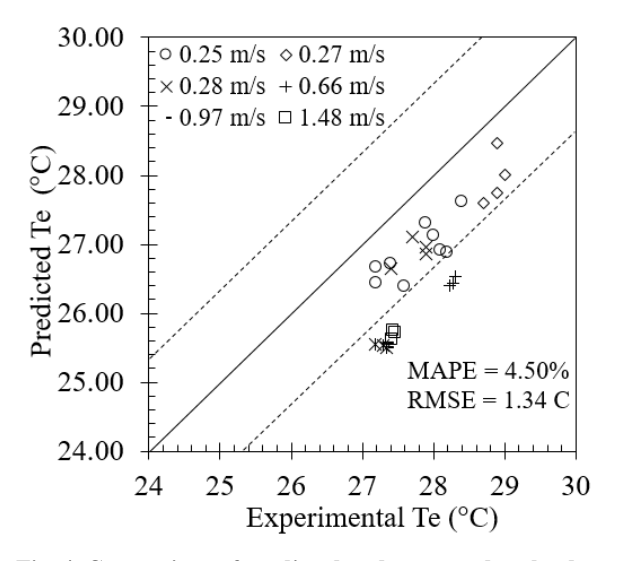


Fig. 4. Comparison of predicted and measured outlet drybulb air temperatures using correlation (8)

3.2 Optimum Pad Thickness Behavior

Simulation results under all conditions listed in Table 1 reveal a consistent trend in the relationship between pad thickness and total cost, which exhibits a characteristic U-shaped curve. To illustrate this behavior more clearly, a representative case is selected with the following parameters: inlet air temperature of 32 °C, wet-bulb depression of 4 °C, pad specific surface area of $400 \, \text{m}^2\text{m}^{-3}$, conditioned space volume of $150 \, \text{m}^3$, and $\alpha = 0.0112$. The corresponding results are shown in Figure 6.

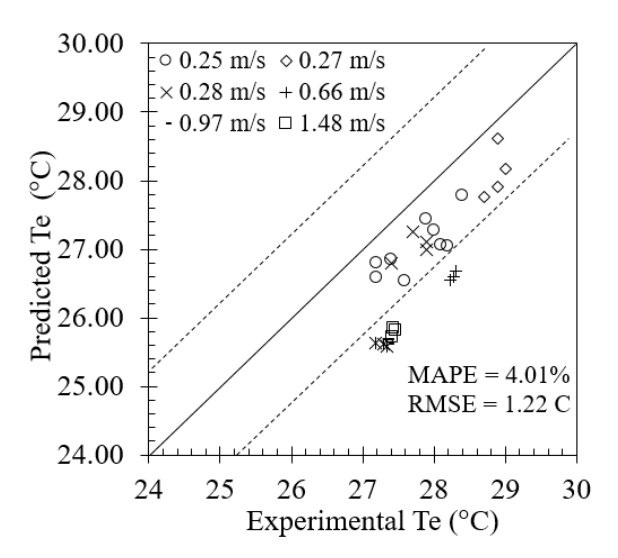


Fig. 5. Comparison of predicted and measured outlet drybulb air temperatures using correlation (9).

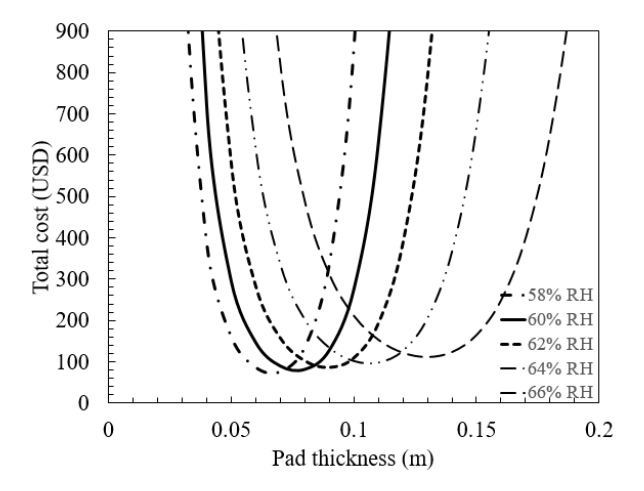


Fig. 6. Relationship between pad thickness and total cost.

At a relative humidity of 58%, the total cost components at a pad thickness of 0.04 m are as follows: pad material cost of 190.51 USD, pump electricity cost of 197.15 USD, and fan electricity cost of 0.73 USD. At the bottom of the U-curve, where the total cost is minimized (at 0.07 m pad thickness), the respective costs are reduced to 26.37 USD, 15.60 USD, and 34.21 USD. The region between 0.04 m and 0.07 m lies on the left-hand side of the U-curve, where both pad material cost and pump electricity cost decrease significantly with increasing pad thickness. Thinner pads require a larger cross-sectional area to ensure sufficient heat exchange, leading to higher material and water consumption, which increases both the pad cost and the energy required to operate the water pump. However, a thinner pad also results in lower airflow resistance, reducing the fan power consumption and associated electricity cost.

Beyond the optimum point, as the pad thickness increases further to 0.10 m, the costs shift significantly: pad material cost drops to 7.48 USD, pump electricity cost to 3.10 USD, while the fan electricity cost rises sharply to 851.56 USD. This region corresponds to the right-hand side of the U-curve, where the increased

airflow resistance from thicker pads leads to a dramatic rise in fan energy consumption, dominating the total cost. These findings demonstrate that the minimum total cost occurs at an intermediate pad thickness—thick enough to reduce pad and pump costs, but not so thick as to excessively increase fan power requirements. This specific thickness is defined as the optimum pad thickness, where the combined costs are minimized.

The emergence of this optimum point is the result of a trade-off between two opposing cost trends: (1) decreasing costs for the pad material and pump operation with increasing pad thickness, and (2) increasing fan electricity cost with increasing thickness due to higher pressure drop. This competitive dynamic always produces a cost-minimizing point, a behavior that aligns with similar optimization findings in thermal insulation for HVAC systems [22] and refrigeration systems [23].

This cost-minimization behavior was consistently observed across all simulation cases in this study. Therefore, it can be concluded that for cellulose corrugated pads used in direct evaporative cooling systems, there always exists an optimum pad thickness at which the total cost is minimized.

3.3 Sensitivity Analysis of Parameters

The sensitivity analysis of the parameters affecting the optimum thickness change of the wetted pad was conducted based on the following reference case: conditioned space volume of 150 m³, inlet air temperature of 31°C, outlet air temperature of 28 °C, relative humidity of 58%, air change rate of 30 ACH, specific surface area of the pad of 400 m²m⁻³, pad material cost of 352.08 USD-m⁻³, and electricity cost of 3.94 USD-kWh⁻¹. Under these conditions, the calculated optimum thickness of the wetted pad was 35.8 mm. The sensitivity analysis was performed by varying each parameter by 5% and 10%.

As shown in Figure 7, which depicts the relationship between optimum thickness variation and the associated parameters, the sensitivity analysis reveals that temperature-related variables exert the greatest influence on the optimum thickness change of cellulose pads. Specifically, when the inlet air temperature and outlet air temperature vary by $\pm 10\%$, the optimum thickness changes in the ranges of approximately 52-213 mm and 24-211 respectively. These variations are substantially larger than those of other parameters, demonstrating that even minor changes in temperature can lead to considerable deviations in the design outcome. In contrast, relative humidity exerts a moderate influence, causing only about a 5-15 mm change in optimum thickness under the same $\pm 10\%$ variation.

Conversely, other factors such as room volume, air change per hour, unit pad cost, and electricity cost have almost negligible effects, with deviations not exceeding 0.1 mm even under $\pm 10\%$ parameter changes. The specific surface area exhibits a small but noticeable impact, with variations limited to about 2–5 mm.

Therefore, it can be concluded that the optimum thickness design of cellulose pads is primarily governed by temperature-related parameters, while economic and operational factors contribute only marginal effects.

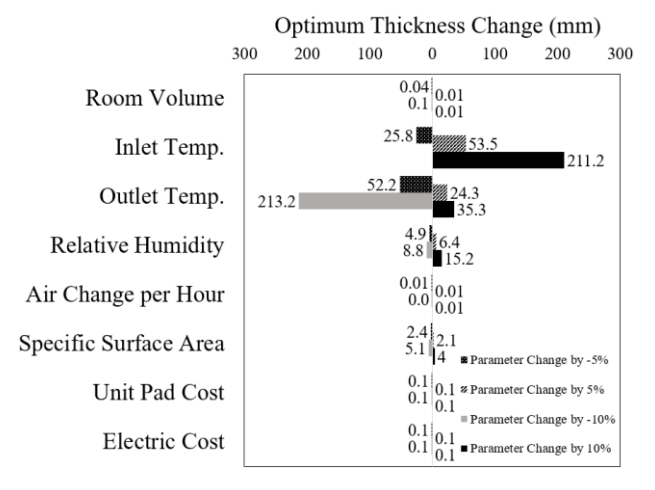


Fig. 7. Sensitivity analysis of parameters affecting the optimum thickness change.

3.4 Correlation for Predicting Optimum Pad Thickness

According to the computational procedure outlined in Section 2.1.1, the saturation effectiveness is determined from the inlet air temperature, relative humidity, and wet-bulb depression, which are prescribed as initial input conditions in the simulation. Consequently, the saturation effectiveness inherently captures both inlet and outlet air states and can thus serve as a representative indicator of climatic conditions. On this basis, the formulation of a predictive correlation for optimum pad thickness begins with an examination of the relationship between ambient conditions and the optimum thickness, using saturation effectiveness as the connecting variable. Figures 8–10 present this relationship for three different specific surface areas of the cellulose corrugated pad, namely 370, 400, and 420 m²m⁻³. The results reveal that the optimum pad thickness follows a trend describable by a composite of two cubic polynomial functions with respect to saturation effectiveness. A polynomial regression of this trend provides a generalized correlation expressed as follows:

$$L_{op} = a_4 \varepsilon^3 + a_3 \varepsilon^2 + a_2 \varepsilon + a_1 \tag{24}$$

In this correlation, ε represents the saturation effectiveness, while a₁ through a₄ are the regression coefficients. Their numerical values, together with the coefficient of determination (R²), root mean square error (RMSE), mean absolute percentage error (MAPE), and the applicable range of saturation effectiveness, are provided in Table 2. As indicated, the predictive model demonstrates reliable performance across the range of 0.45–0.90 for all examined pad specific surface areas, with both RMSE and MAPE remaining at suitably low levels. At higher saturation effectiveness values (0.90–0.99), however, the MAPE increases to 19.44%,

suggesting that predictions in this region should be treated with caution.

To evaluate the applicability range of the proposed correlation, the effects of conditioned space volume, air changes per hour (ACH), and the cost factor (α) on the predicted optimum pad thickness were analyzed. The findings are illustrated in Figures 11 through 13. As shown in Figure 11, the predicted optimum pad

thickness exhibits a deviation of no more than 12% for room volumes ranging from 15 to 1,500 m³. However, when the room volume increases to 15,000 m³, the prediction error reaches 37.5%, which exceeds an acceptable threshold. Therefore, the recommended range of room volumes for the use of this correlation is 15–1,500 m³.

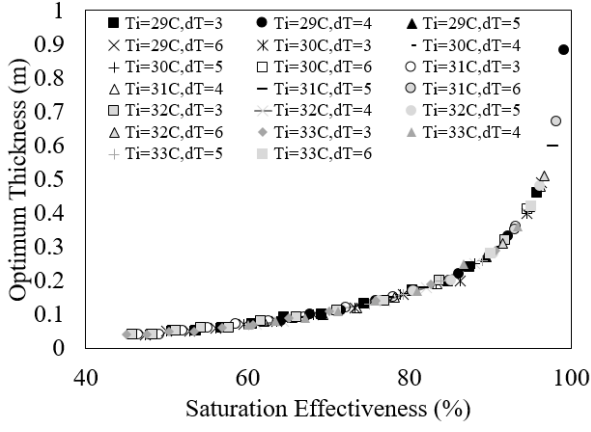


Fig. 8 Relationship between optimum pad thickness and saturation effectiveness for a specific surface area of $370 \text{ m}^2\text{m}^{-3}$.

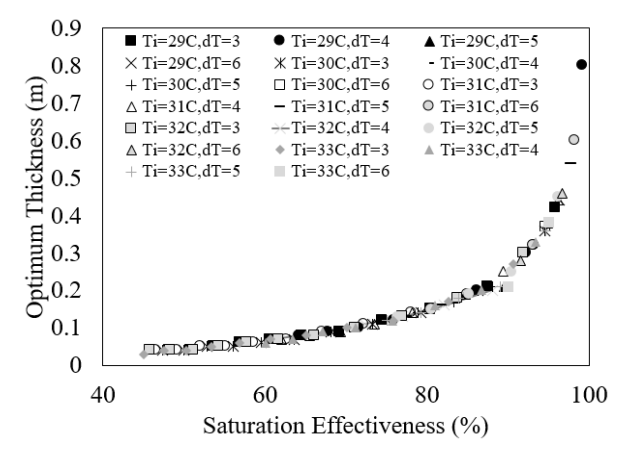


Fig. 9. Relationship between optimum pad thickness and saturation effectiveness for a specific surface area of $400 \text{ m}^2\text{m}^{-3}$.

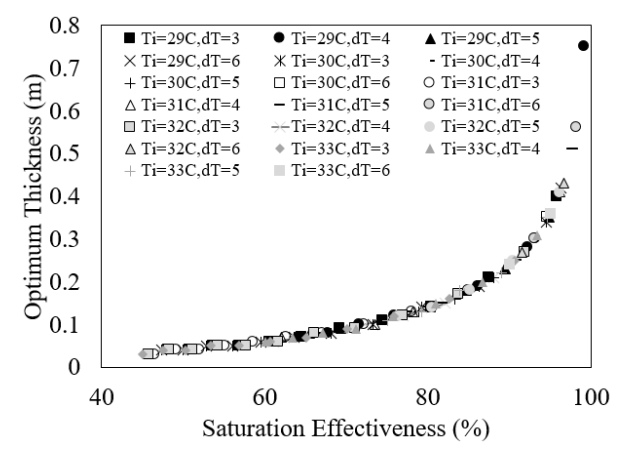
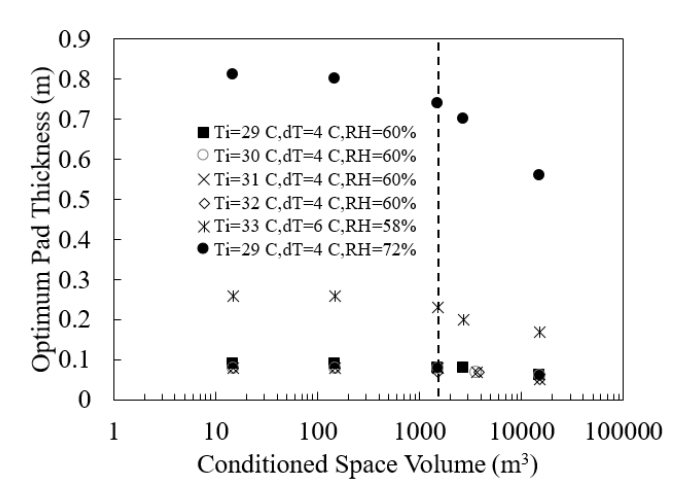


Fig. 10. Relationship between optimum pad thickness and saturation effectiveness for a specific surface area of $420~\text{m}^2\text{m}^{-3}$.

Table 2. Polynomial regression coefficients and performance metrics for predicting optimum pad thickness.

Applicable	a4	a ₃	$\mathbf{a_2}$	$\mathbf{a_1}$	\mathbb{R}^2	RMSE	MAPE
range						(m)	(%)
$A_s=370 \text{ m}^2\text{m}^{-3}$	2.9312	-4.7997	2.8518	-0.5454	0.9942	0.0049	0.033
$0.45 < \epsilon < 0.90$							
$A_s=370 \text{ m}^2\text{m}^{-3}$	1489.3	-4154.6	3865.5	-1199.2	0.9944	0.0261	6.025
$0.90 < \epsilon < 0.99$							
$A_s=400 \text{ m}^2\text{m}^{-3}$	1.2019	-1.5609	0.8335	0.134	0.9916	0.0051	0.036
$0.45 < \epsilon < 0.90$							
A_s =400 m ² m ⁻³	1359.9	-3794.2	3530.7	-1095.4	0.9919	0.0721	19.44
0.90< €<0.99							
$A_s=420 \text{ m}^2\text{m}^{-3}$	2.656	-4.3617	2.5774	-0.4893	0.9965	0.0033	0.034
0.45<ε<0.90							
A_s =420 m ² m ⁻³	1184.2	-3298.9	3065	-949.51	0.9916	0.0638	18.00
0.90<ε<0.99							

©2025. Published by RERIC in International Energy Journal (IEJ), selection and/or peer-reviewed under the responsibility of the Organizers of the "17th International Conference on Science, Technology and Innovation for Sustainable Well-Being (STISWB 2025)" and the Guest Editor: Prof. Pradit Terdtoon of Chiang Mai University, Chiang Mai, Thailand.



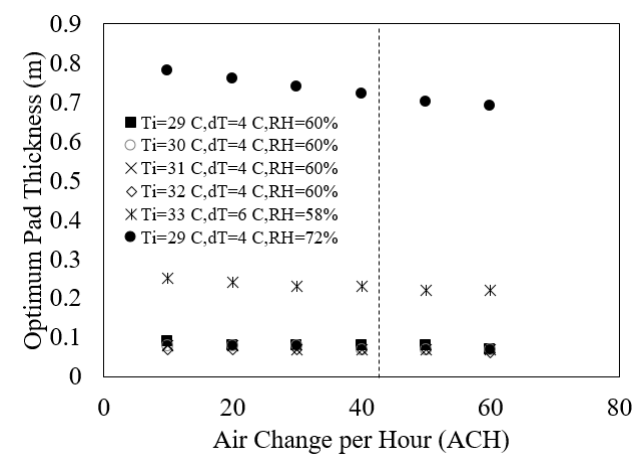


Fig.11. Variation of optimum pad thickness with conditioned space volume.

Fig. 12. Variation of optimum pad thickness with air change per hour at Vroom = 1,500 m³.

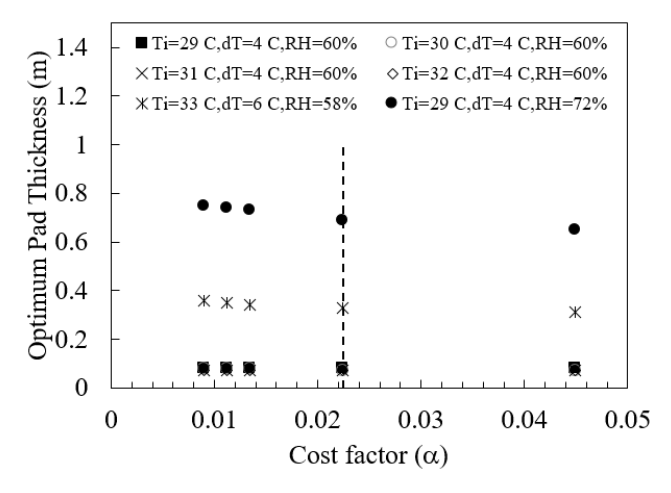


Fig. 13. Variation of Optimum Pad Thickness with Cost factor (α) at Vroom = 1,500 m³.

Similarly, Figures 12 and 13 indicate that the correlation yields prediction errors of no more than 12.5% and 8.3% for ACH values between 10–40 h^{-1} and α values between 0.0090–0.0224, respectively. Since the parameter α reflects the relative cost of materials and energy, these findings suggest that variations in the cost of pad materials or electricity—within the specified α range—will have a negligible impact on the predicted optimum pad thickness.

4. CONCLUSIONS

This study developed a comprehensive mathematical model to determine the optimum thickness of cellulose corrugated wetted pads in direct evaporative cooling systems. The model incorporates heat transfer performance, airflow pressure drop, and overall system cost, considering the influence of inlet air temperature, relative humidity, and wet-bulb depression. The proposed model accurately predicted the outlet air temperature, achieving a minimum RMSE of 1.22 °C and a MAPE of 4.01% when validated against experimental data. Furthermore, the relationship between pad thickness and total system cost exhibited a characteristic U-shaped trend, indicating an optimal point where the combined cost of pad materials, pump

energy, and fan power is minimized. The sensitivity analysis revealed that inlet air temperature and outlet air temperature are the most influential parameters affecting the optimum wetted pad thickness. Hence, careful consideration of these parameters is essential to ensure accurate determination of the optimum design. To enable rapid estimation of the optimum pad thickness without resorting to computationally intensive bruteforce approaches, a third-degree polynomial correlation was developed using saturation effectiveness as the independent variable. The correlation showed high predictive accuracy within an effectiveness range of 0.45-0.90, with MAPE values below 4% and RMSE below 0.005 m across all examined specific surface areas. However, for saturation effectiveness values above 0.90, prediction errors increased significantly, reaching a MAPE of 19.44%, suggesting that the correlation should be applied with caution in this range. The applicability limits of the proposed correlation were further evaluated. Reliable predictions were achieved for room volumes between 15-1,500 m³, ACH values between 10-40 h⁻¹, and cost factor (α) values ranging from 0.0090 to 0.0224, with prediction errors remaining within 12.5%. It is important to note that the predicted optimum thickness derived from the developed correlation serves primarily as a tool to avoid brute-force optimization. Detailed cost analyses—incorporating fan, pump, structural components, maintenance, and other operational costs—remain essential for making fully informed design decisions. For saturation effectiveness values above 0.9, future research should explore alternative relationships beyond polynomial regression to achieve higher accuracy within this range.

ACKNOWLEDGEMENT

The authors would like to express their sincere appreciation to the Silpakorn University Research, Innovation, and Creative Fund, as well as the Department of Mechanical Engineering, Faculty of Engineering and Industrial Technology, Silpakorn University, Sanam Chandra Palace Campus, for their generous support.

NOMENCLATURE

 $A_{\rm w}$ heat transfer area (m²) specific area of wet pad (m²) A_s A_{pad} cross section area of wet pad (m²) ACH air change per hour (h⁻¹) total cost (USD) $Cost_{total} \\$ cost of wet pad (USD) Cost_{pad} electricity cost of fan (USD) $Cost_{E,fan}$ $Cost_{E,pump}$ electricity cost of pump (USD) electrical energy consumption of fan (kWh) E_{fan} electrical energy consumption of pump (kWh) E_{pump} L wet pad thickness (m) characteristic length (m) Le $L_{\text{op}} \\$ optimum pad thickness (m) ΔP_{drop} air pressure drop (Pa) water flow rate (m³h⁻¹) $Q_{\rm w}$ RH relative humidity (%) T_{WB} wet bulb temperature (°C) T_{i} dry bulb temperature of inlet air (°C) T_e dry bulb temperature of outlet air (°C) V_{pad} volume of wet pad (m³) V_{room} conditioned space volume (m³) constant pressure specific heat of air $c_{p,air}$ $(J kg^{-1}K^{-1})$ convective heat transfers coefficient h_c $(W m^{-2} K^{-1})$ h work hours (h) $k_{\text{pad}} \\$ price of wet pad per unit volume (USD m⁻³) unit price of electricity (USD unit⁻¹) $k_{\rm E}$ air thermal conductivity (W m⁻¹K⁻¹) k_{air} \dot{m}_{air} mass flow rate of air (kg s⁻¹) specific water flow rate (m³ h⁻¹m⁻²) $q_{\rm w}$ air velocity (m s⁻¹) α cost factor saturation effectiveness 8.

fan efficiency

pump efficiency

 η_{fan}

 η_{pump}

 $\begin{array}{ll} \rho_{air} & \text{air density (kg m}^{-3}) \\ \mu & \text{dynamic viscosity (Pa-s)} \\ \text{Nu} & \text{Nusselt number} \\ \text{Pr} & \text{Prandtl number} \\ \text{Re} & \text{Reynolds number} \end{array}$

REFERENCES

- [1] Oropeza-Perez I. and P.A. Østergaard. 2018. Active and passive cooling methods for dwellings: A review. *Renewable and Sustainable Energy Reviews* 82: 531-544. doi: 10.1016/j.rser.2017.09.059.
- [2] Watt J.R. 1986. Evaporative Air Conditioning Handbook, 2nd ed. Boston, MA, USA: Springer US. doi: 10.1007/978-1-4613-2259-7.
- [3] Ghani S., Bakochristou F. ElBialy E.M.A.A., Gamaledin S.M.A., Rashwan M.M., Abdelhalim A.M., and Ismail S.M., 2019. Design challenges of agricultural greenhouses in hot and arid environments A review. *Engineering in Agriculture, Environment and Food* 12: 48–70. doi: 10.1016/j.eaef.2018.09.004.
- [4] Al Assaad D.K., Orabi M.S., Ghaddar N.K., Ghali K.F., Salam D.A., Ouahrani D., Farran M.T., and Habib R.R., 2021. A sustainable localised air distribution system for enhancing thermal environment and indoor air quality of poultry house for semiarid region. *Biosystems Engineering* 203: 70-92. doi: 10.1016/j.biosystemseng.2021.01.002.
- [5] Xuan Y.M., Xiao F., Niu X.F., Huang X., and Wang S.W., 2012. Research and application of evaporative cooling in China: A review (I) – Research. Renewable and Sustainable Energy Reviews 16: 3535–3546. doi: 10.1016/j.rser.2012.01.052.
- [6] Ulpiani G., 2019. Water mist spray for outdoor cooling: A systematic review of technologies, methods and impacts. *Applied Energy* 254: 113647. doi: 10.1016/j.apenergy.2019.113647.
- [7] Pérez-Urrestarazu L., Fernández-Cañero R., Franco A., and Egea G., 2016. Influence of an active living wall on indoor temperature and humidity conditions. *Ecological Engineering* 90: 120–124. doi: 10.1016/j.ecoleng.2016.01.050.
- [8] Watson J.A., Gómez C., Bucklin R.A., Leary J.D., and McConnell D.B., 2019. Fan and pad greenhouse evaporative cooling systems. *Univ.* Florida IFAS Extension, 2019. [Online]. Available: https://edis.ifas.ufl.edu/publication/AE069
- [9] Franco A. and D.L. Valera. 2014. Energy efficiency in greenhouse evaporative cooling: Cooling boxes versus cellulose pads. *Energies* 7(3): 1427–1447. doi: 10.3390/en7031427.
- [10] Ahmed E.M., Abaas O., Ahmed M., and Ismail M.R., 2011. Performance evaluation of three different types of local evaporative cooling pads in greenhouses in Sudan. *Saudi Journal of Biological*

- Sciences 18(1): 45–51. doi: 10.1016/j.sjbs.2010.09.005.
- [11] Czarick M. and B. Fairchild. 2012. Plastic less effective than paper evaporative cooling pads! *World Poultrymeat* 28: 26–29.
- [12] Martínez P., Ruiz J., Martínez P.J., Kaiser A.S., and Lucas M., 2018. Experimental study of the energy and exergy performance of a plastic mesh evaporative pad used in air conditioning applications. *Applied Thermal Engineering* 138: 675–685. doi: 10.1016/j.applthermaleng.2018.04.065.
- [13] Liao C.M. and K.H. Chiu. 2002. Wind tunnel modeling the system performance of alternative evaporative cooling pads in Taiwan region. *Building Environment* 37: 177–187. doi: 10.1016/S0360-1323(00)00098-6.
- [14] Franco A., Valera D.L., Madueño A., and Peña A., 2010. Influence of water and air flow on the performance of cellulose evaporative cooling pads used in Mediterranean greenhouses. *Transactions of ASABE* 53(2): 565–576.
- [15] A. Malli, Seyf H.R., Layeghi M., Sharifian S., and Behravesh H., 2011. Investigating the performance of cellulosic evaporative cooling pads. *Energy Conversion and Management* 52(6): 2598–2603. doi: 10.1016/j.enconman.2010.12.015.
- [16] Doğramacı P.A., Riffat S., Gan G., and Aydın D., 2019. Experimental study of the potential of eucalyptus fibres for evaporative cooling. *Renewable Energy* 131: 250–260. doi: 10.1016/j.renene.2018.07.005.
- [17] Nada S.A., Fouda A., Mahmoud M.A., and Elattar H.F., 2019. Experimental investigation of energy and exergy performance of a direct evaporative cooler using a new pad type. *Energy and Buildings* 203: 109425. doi: 10.1016/j.enbuild.2019.109425.
- [18] Barzegar M., Layeghi M., Ebrahimi G., Hamzeh Y., and Khorasani M., 2012. Experimental evaluation of the performances of cellulosic pads made out of Kraft and NSSC corrugated papers as evaporative media. *Energy Conversion and. Management* 54: 24-29. doi: 10.1016/j.enconman.2011.09.018.
- [19] Naveenprabhu V. and M. Suresh. 2020. Performance enhancement studies on evaporative cooling using volumetric heat and mass transfer coefficients. *Numerical Heat Transfer* 7899): 504-523. doi: 10.1080/10407782.2020.1793556.
- [20] Elmsaad E.M.A.Y., Elnewiry O.A.M., and Ali M.A., 2017. Impact of different thicknesses of evaporative cooling pads on crop yield in greenhouse. *International Journal of Agriculture Innovation and Research* 5(5): 883–888.
- [21] Rashwan M.A., Al-Helal I.M., Al-Kahtani S.M., Alkoaik F.N., Fickak A.A., Almasoud W.A., Alshamiry F.A., Ibrahim M.N., Fulleros R.B., and Shady M.R., 2025. Performance evaluation of volcanic stone pad used in evaporative cooling

- system. *Energies* 18(8):1897. doi: 10.3390/en18081897.
- [22] Soponpongpipat N., Jaruyanon P., and Nanetoe S., 2010. The thermo-economics analysis of the optimum thickness of double-layer insulation for air conditioning duct. *Energy Research Journal* 1(2): 146–151. doi: 10.3844/erjsp.2010.146.151.
- [23] Soylemez M.S. and M. Unsal. 1999. Optimum insulation thickness for refrigeration applications. *Energy Conversion and Management* 40(1): 13-21.
- [24] Bishoyi D. and K. Sudhakar. 2017. Experimental performance of a direct evaporative cooler in composite climate of India. *Energy and Buildings* 153: 190-200. doi: 10.1016/j.enbuild.2017.08.018.
- [25] Stull R., 2011. Wet-bulb temperature from relative humidity and air temperature. *Journal of Applied Meteorology and Climatology* 50(11): 2267-2269.
- [26] Camargo J.R., Ebinuma C.D., and Silveira J.L., 2005. Experimental performance of a direct evaporative cooler operating during summer in a Brazilian city. *International Journal of Refrigeration* 28(7): 1124-1132. doi: 10.1016/j.ijrefrig.2004.12.011.
- [27] He S., Guan Z., Gurgenci H., Jahn I., Lu Y., Alkhedhair A.M., 2014. Influence of ambient conditions and water flow on the performance of pre-cooled natural draft dry cooling towers. *Applied Thermal Engineering* 66: 621–631. doi: 10.1016/j.applthermaleng.2014.02.070.
- [28] Kulkarni R.K. and S.P.S. Rajput. 2013. Comparative performance analysis of evaporative cooling pads of alternative configurations and materials. *International Journal of Advance Engineering Technology* 6(4): 1524–1534.
- [29] Sonntag D.B., Jung H., Harline R.P., Peterson T.C., Willis S.E., Christensen T.R., and Johnston J.D., 2024. Infiltration of Outdoor PM2.5 Pollution into Homes with Evaporative Coolers in Utah County. *Sustainability* 16(1): 177. doi: 10.3390/su16010177.
- [30] Itani M., Ghali K., and Ghaddar N., 2015. Increasing energy efficiency of displacement ventilation integrated with an evaporative-cooled ceiling for operation in hot humid climate. *Energy* and *Buildings* 105: 26-36. doi: 10.1016/j.enbuild.2015.07.045.
- [31] Martínez P.J., et al., 2024. Analytical modelling of an indirect evaporative cooler based on the Mcycle," in *Proc. CYTEF 2024, XII Congreso Ibérico de las Ciencias y Técnicas del Frío*, 2024.
- [32] National Renewable Energy Laboratory (NREL), 2012. Development and analysis of a desiccant-enhanced evaporative air conditioner prototype. NREL/TP-5500-54755.
- [33] Ghoname M.S., 2020. Effect of pad water flow rate on evaporative cooling system efficiency in laying hen housing. *Journal of Agricultural Engineering* 51(4), 213–218.